Abrasive Blasting Contamination in Super Duplex and Carbon Steels – a Quantification Approach by Rietveld Analysis

Adriana da Cunha Rocha*, Áquila Vieira do Nascimento, Isabel Cristina Pereira Margarit-Mattos,

Kioshy dos Santos Assis, Oscar Rosa Mattos

*Non-Destructive Tests Corrosion and Welding Laboratory – LNDC, Alberto Luiz Coimbra Institute
Graduate School and Research in Engineering – COPPE, Federal University of Rio de Janeiro – UFRJ,
Rua Pedro Calmon, s/n, CEP 21941-596, Rio de Janeiro, RJ, Brazil*

A methodology for quantifying the contamination after abrasive blasting by Aluminum Oxide and Martensitic Carbon Steel particles in Super Duplex and Carbon Steel substrates has been developed. The method consisted of performing x-ray diffraction in the blasted steel substrates and calculating the particle contamination using Rietveld Quantitative Method. In this way, it is possible to evaluate the substrate volume in which the abrasive particles have been trapped (taking into account the surface roughness) rather than solely performing visual examination, as indicated by standards documents. Equations describing the intensity model of the diffracted peaks as well as those describing the quantitative measurements are presented. Correction functions are also employed to compensate the effect of the surface roughness generated on the metallic substrates after blasting. Alumina and martensitic steel abrasives contaminations were detected and quantified in both steel substrates. Results showed that Super Duplex Steel substrates revealed a higher degree of contamination when compared to the Carbon Steel substrates, both for alumina abrasives as for martensitic abrasives. Also, the abrasive that generated the lower degree of contamination was the Martensitic Carbon Steel, for both substrates.

keywords: *x-ray diffraction, Rietveld method, Duplex Stainless Steel, abrasive contamination*

1. Introduction

Duplex and super duplex steels (DS and SDS respectively) have been widely used in oil and gas industry where the need for materials with good mechanical properties, as well as good corrosion resistance is ultimate[1-3]. These steels do indeed present satisfactory corrosion behavior but, due to the increasing of aggressive environments to which those steels have been subjected to they need to be, somehow, protected from degradation as they eventually will lose their resistance to corrosion.

A good alternative for this type of protection is found in organic coatings[4,5]. The effectiveness of such coatings is dependent not only on the properties of the coatings but also on the character of the metal substrate, the surface pretreatment and the application procedures[6,7].

The surface preparation should be in accordance with specifications defined by standards documents[8,9], which include procedures for blast cleaning. The coating adhesion and corrosion rate are highly influenced by the degree of contamination that might exist in a surface after blasting processes. Such contamination is mostly by particulates of the abrasive itself that might create local pH changes and/ or galvanic effects when the substrate is, exposed to the corrosion environment[10].

Super duplex steels, in comparison with iron steels, present high values of hardness and high electrochemical

potentials. Therefore, the choice of abrasives for surface treatment needs to take these features into account. Aluminum oxide and martensitic steels abrasives are good choices for this purpose. Aluminum oxide grit has high value of hardness but the grit dimension does not maintain itself and usually pulverizes during blasting. Moreover, depending on the origin of the aluminum oxide, it can induce surface alkalization, leading thus to a decrease in the corrosion protection characteristics of the coating. Martensitic abrasives incrustations, however, can promote corrosion by galvanic action with the steel substrate if the electrochemical potential of the grit differs from that of the substrate[10].

Hence, substrate contamination needs to be addressed in a trustable way in order to optimize the blasting parameters avoiding abrasives that impair performance of the whole system. The most used method of quantifying this contamination is by visual metallographic analysis and, more specifically, by determining the inclusion or second-phase constituent content of substrates[11]. This technique can be performed by image analysis, but even in the automatic way, the technique itself requires a large number of measurements to be statistical accurate, what can be quite time consuming. Also, depending on the case, visual distinction between the substrate and the incrustation can be very hard or even impossible.

*e-mail: adrirocha@metalmat.ufrj.br

An alternative for the quantification of the abrasive contamination is found in Quantitative Phase Analysis (QPA) by X-ray Diffraction. Quantitative determination of phases in a multi-component polycrystalline mixture is a basic goal in materials characterization[12]. Many methods have been developed for performing this quantification through x-ray diffraction, but none of them can completely overcome systematic errors like peak overlapping, preferred orientation and micro absorption effects[13-16]. Because of several advantages compared with traditional internal-standard-based techniques, the Rietveld Method[17] has been applied to such task and it has been used to systems of gradually increasing complexity, either in terms of number of phases, structure complexity or degree of structure order. These applications have shown that Rietveld analysis can provide very accurate estimative of the relative and/or absolute abundance of the component phases[17-22].

This work presents a methodology for determining the contamination of alumina and martensitic steel abrasive blasting in super duplex and carbon steel substrates, by means of x-ray diffraction using the Rietveld quantitative method. A way of identifying and quantifying this type of contamination is provided and the term "degree of contamination" is used in respect to the volume ration of abrasive particles phases in relation to the substrate phases. The advantage of this method is that, by utilizing x-ray diffraction, it is possible to evaluate the substrate volume in which the abrasive particles are trapped. This is an important complement to the visual examination that is usually indicated by standards documents as one of the methods to assess this type of contamination.

Equations describing the intensity model as well as those describing the quantitative measurements are presented. Surface roughness effects were also taken into account and compensated by the use of correction functions proposed by Suortti[23]. Results are based on the analysis performed by Diffrac Plus TOPAS 4.2[24].

2. Material and Methods

2.1. The quantitative phase analysis and the rietveld method

In the Rietveld method[25] least-squares refinements are carried out until the best fit is obtained between the entire observed powder diffraction pattern and the full calculated pattern. The quantity minimized in the least-squares refinement is the residual S_y :

$$S_y = \sum_i w_i (y_i - y_{ci})^2 \qquad (1)$$

Where y_i is the observed (gross) intensity at the i th step, y_{CI} is the calculated intensity at the i th step, $w_I = 1/y_I$ and the sum is overall data points.

The method has as its basic premise that no efforts should be made in advance to allocate observed intensity to particular Bragg reflections or to resolve overlapped reflections. Therefore, it is necessary that a good starting model is used. In this case, different Bragg reflections contributing to a specific intensity y_I are taken into account at every specific i point in the whole pattern. The calculated intensities can be performed considering the structure factor F_K, for the Kth Bragg reflection. This is done by summing of the calculated contributions from neighbouring Bragg reflections (within a specific range) plus the background, as described in Equation 2.

$$y_{ci} = s \sum_K L_K \left| F_K \right|^2 \varnothing (2\Theta_i - 2\Theta_k) P_K A + y_{bi} \qquad (2)$$

Where s is the scale factor, K represents the Miller indices, h, k, l for a Bragg reflection, L_K contains the Lorentz polarization and multiplication factors, $\varnothing$ is the reflection profile function, P_K is the preferred orientation function, A is an absorption factor, $|F_K|$ is the structure factor modulus for the Kth Bragg reflection, y_{BI} is the background intensity at the ith step.

In the QPA[25-27] using the Rietveld method, the relative weight fraction W of each phase p in a mixture of n phases is calculated according to the equation:

$$W_p = (s_p\, ZMV) / \sum_{i=1}^{n} s_i\, (ZMV)_i \qquad (3)$$

Where S is the Rietveld scale factor, Z is number of formula units per unit cell, M is the mass of the formula unit (in atomic mass units) and V is the unit cell volume (in Å^3).

In this way, when analyzing a specific volume of material, it is possible to determine the amount of components in that volume. Thus, when analyzing a finite volume of metallic substrate subjected to abrasive blasting, it is possible to calculate by QPA the volume percentage of particles that might have been deposited in that finite volume.

2.2. Surface roughness corrections

In Rietveld analysis of X-ray powder diffraction patterns obtained using Bragg-Brentano reflection geometry, the effect of surface roughness (SR) of absorbing polycrystalline samples can be a source of systematic errors[28,29]. To correct this type of inconsistencies, three empirical SR correction functions are commonly used in the Rietveld method, being the SR Sparks Model[29], the SR Pitschke Model[30,31] and the SR Suortti Model[23]. In this work the Suortti Model was chosen due to its higher flexibility in terms of angular ranges[32,33].

2.3. Experimental parameters

Carbon Steel (CS) and Super Duplex Steel (SDS) samples were used as metallic substrates subjected to the blasting process. The chemical composition and the hardness values of each substrate are given in Table 1.

Table 1. Chemical Composition (wt%) and Vickers Hardness Values (HV) of Carbon Steel and Super Duplex Steel Substrates.

Steel Chemical Composition (wt%)	C	Mn	Cr	Mo	Ni	Si	N	Cu	HV
Carbon Steel ASTM A516[34]	0.169	0.780				0.178	0.20		126
Super Duplex Steel UNS 32760	0.03	0.55	24.45	3.74	7.06		0.20	0.53	224

The abrasives used encompassed two types of aluminum oxide particulate (sintered bauxite (SB) and demagnetized alumina (DA)) and two types of martensitic steel grit (martensitic stainless steel (MSS) and martensitic carbon steel (MCS)). The chemical composition of each type of abrasive is given in Table 2.

The dimensions of the plate-like samples were 45mm × 45mm and they all have a thickness of 4,5mm, approximately. A set of four samples of each different material (CS and SDS) were blasted with each one of the four different types of abrasives, totalizing 32 samples. Abrasive particle size (granulometry) was determine by a Tyler Ro-Tap® 8" Automatic Sieve Shaker, according to the procedures in the ASTM E 11[35] standard and abrasive density was determine through pycnometer method. Hardness measurements on the abrasive particulate were performed on a *Buehler Micromet* 5114 micro hardness machine, according to the ASTM E 384 standard[36]. The results for this experiments are presented in Table 3.

The blasting process was performed with a nozzle diameter of 5/16 inches, using a pressure of 100 psi. The nozzle was positioned at 250 mm from the samples surfaces, in a 90 degree angle. The compressed air utilized was exempt from oil and water. Values for the measured surface roughness, performed by a mechanical rugosimeter (Elcometer 123 Surface Profile Gauge) are listed in Table 4.

Diffraction was performed in a D8 Discover (*Bruker AXS*) using cobalt Co K_α radiation (λ = 1,789Å), equipped with a Lynx Eye PS Detector. The equipment operated at constant values of tension (35 KV) and current (40 mA), respectively.

The primary optics was mounted using a Co Göbel Mirror followed by two slits of 1 mm and 6 mm and a soller slit with an aperture of 2 cm × 1 cm. The secondary optics consisted of a Fe-K_β filter followed by an 8 mm slit and a axial Soller slit with maximum divergence of 2.5°, all mounted in the PSD detector. The scanning data was obtained in the 2θ range of 10° to 110°. The step-size applied was 0.001° and the scanning velocity was 0.5s.step^{-1}.

The Rietveld analysis of each scan was carried out using Diffrac PlusTOPAS (ver 4.2) software, which is a Windows XP, based general non-linear least squares system driven by a scripting language, which focus is in crystallography, solid state chemistry and optimization and, as consequence, has also been applied for quantification through the adoption of the relative weight fraction equation (Equation 3).

The method used for the adjustment of the diffracted peak shapes is the fundamental parameters method, proposed by Cheary and Coelho[37]. This method consists of a convolution approach to X-ray powder line-profile fitting and is developed in a way where the line shape is synthesized from the Co-Kα emission profile, the dimensions of the diffractometer and the physical variables of the specimen. In addition to the integrated intensities and 2θ positions of the line profiles, the parameters that may be fitted include the receiving-slit width, the receiving-slit length, the X-ray-

Table 2. Abrasives Chemical Composition (wt%).

	Al$_2$O$_3$	Fe$_2$O$_3$	SiO$_2$	TiO$_2$	CaO	K$_2$O
Aluminum Oxide Abrasives (wt%)						
Sintered Bauxite (SB)	76.3	14.10	6.2	1.95	0.35	0.49
Demagnetized Alumina (DA)	>89	<3.5	<3.5	<3.5		
Steel Grit Abrasives (wt%)						
	C	Si	Mn	P	S	Cr	Ni
Martensitic Carbon Steel (MCS)	0.8-1.2	<0.4	0.6-102	<0.05	<0.05		
Martensitic Stainless Steel (MSS)	2.0	<2.0	<2.0			30.0	<0.2

Table 3. Average measured values (displayed with calculated standard deviation) for different characteristics of the abrasives. All types of abrasives presented angular morphology.

Abrasive	Density (g.cm^3)	Hardness (HV)	Granulometry (mm)
Sintered Bauxite (SB)	3.65 ± 0.04	1200 ± 30.99	1.0 < 85% < 1.7
Demagnetized Alumina (DA)	3.71 ± 0.01	1236 ± 22.41	1.4 < 85% < 2.0
Martensitic Carbon Steel (MCS)	7.41 ± 0.23	739 ± 23.55	95% > 1.4
Martensitic Stainless Steel (MSS)	7.44 ± 0.07	701 ± 31.39	75% > 1.4

Table 4. Substrates average roughness profiles values (displayed with calculated standard deviation) before and after abrasive blasting process.

Abrasive	Roughness profile values (µm)	
	SDS	CS
Before Blasting	30 ± 12	15 ± 6
SB	112 ± 27	129 ± 19
DA	54 ± 16	67 ± 20
MCS	138 ± 22	142 ± 27
MSS	109 ± 24	119 ± 31

source size, the angle of divergence of the incident beam, the X-ray attenuation coefficient of the specimen and the crystallite size. This is a self-consistent approach to fitting as the instrumental parameters are usually known by direct measurement. To minimize correlation between refined instrumental parameters, profiles at high and low 2θ values were fitted simultaneously.

2.4. Fitting parameters

The structure refinement for the blasted substrates used the fourth-degree Chebyshev Polynomial[38] to fit the background intensities, y_{IB}, according to Equation 2. Also, the 1/x background function, from Topas 4.2, was used to correct background due to air scattering and to allow the use of fewer coefficients in the polynomial function. The zero error (2θ), the sample displacement, the absorption (1/cm) and the lattice parameters of the phases were not fixed and were allowed to vary accordingly in order to provide the best fitting. α−Fe and γ-Fe phases were subjected to the Preferred Orientation (PO) March-Dollase model[39-41] for calculating the preferred crystal orientations that could exist in the substrate. For the alumina phase, PO Spherical Harmonics[42] model of order 6 was used instead, due to the nature of this material, as a particulate. The results for the QPA for the CS and SDS blasted substrates are shown in Figures 1 and 2, respectively.
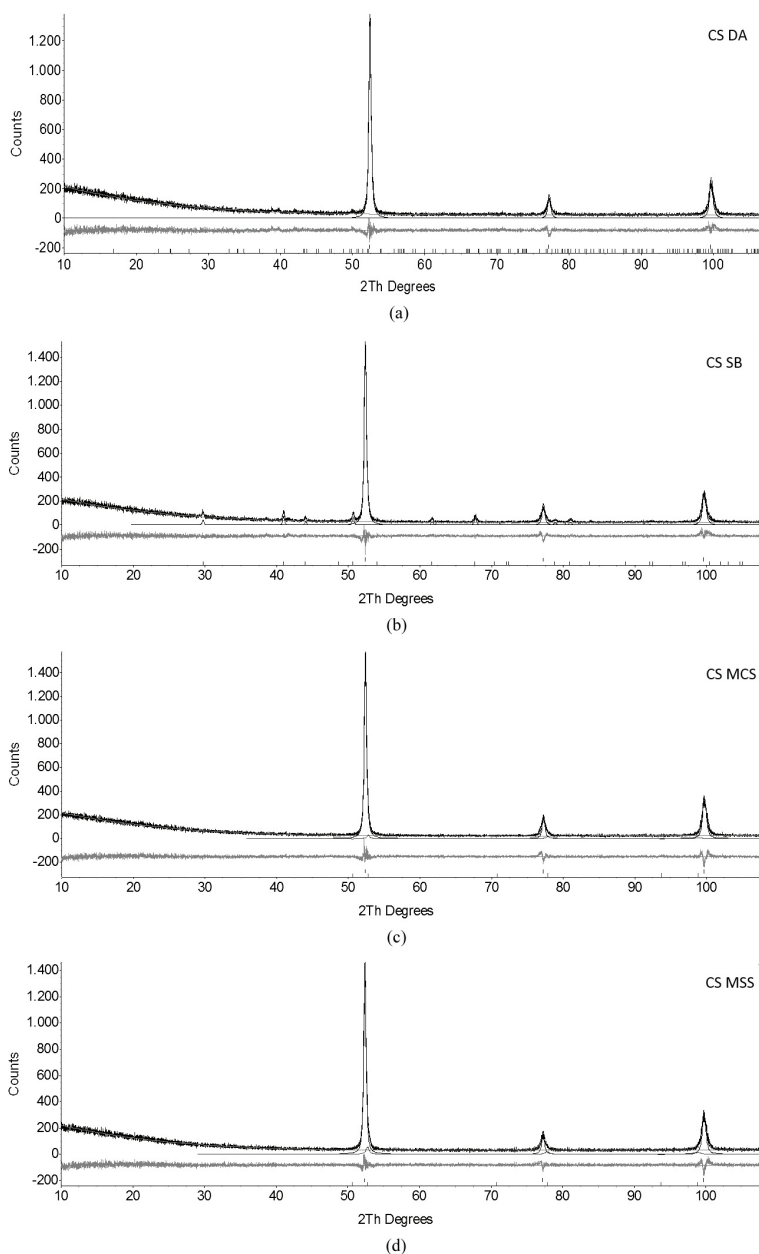

(a)

(b)

(c)

(d)

Figure 1. Rietveld refinement pattern for blasted CS substrate. The observed data are indicated by thicker lines and the calculated data by a solid thinner line just below the observed data. The lower curve shows the difference between the observed and calculated powder diffraction patterns. Carbon steel substrate blasted with (a) DA, (b) SB, (c) MCS and (d) MSS abrasives.
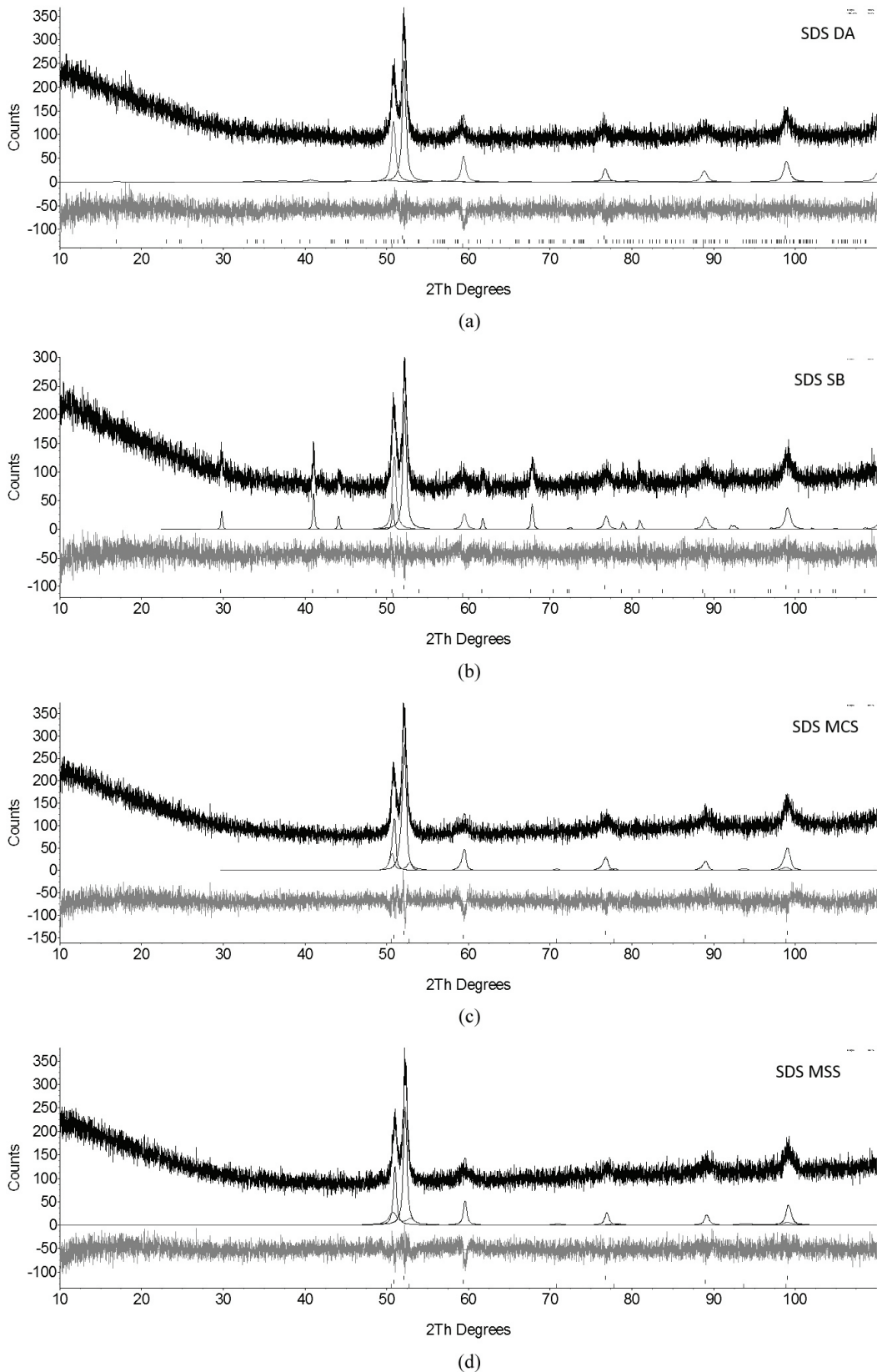
Figure 2. Rietveld refinement pattern for blasted SDS substrate. The observed data is indicated by thicker lines and the calculated data by a solid thinner line just below the observed data. The lower curve shows the difference between the observed and calculated powder diffraction patterns. Super Duplex steel substrate blasted with (a) DA, (b) SB, (c) MCS and (d) MSS abrasives.

2.5. Fitting criteria

When Rietveld calculations are performed, it is also necessary to address a way of analyzing the efficiency of the fittings. The fitting criteria used are based on the R-values, which are the criteria developed from the crystallography for Rietveld Analysis[43-45]. In this case, the R-weighted pattern (R_{wp}) and the R-expected pattern (R_e) are the ones employed (Equations 4 and 5). Also, another numerical criterion, the "goodness of fit", or simply GOF (Equation 6), is used as a way of addressing the values obtained after the fitting calculations are performed.

$$R_{wp} = [(\sum wi \, (yi \, (obs) - yi \, (calc))^2) / (\sum wi \, (yi \, (obs)^2))]^{1/2} \quad (4)$$

$$R_{exp} = [(N\text{-}P) / (\sum wi \, (yi \, (obs)^2))]^{1/2} \quad (5)$$

$$GOF = [(S_Y) / (N\text{-}P)]^{1/2} = R_{wp}/R_{exp} \quad (6)$$

Where, y_I = intensity at the i-th step, w_I = weighting factor, N = number of observations, P = number of parameters, **obs** = observed and **calc** = calculated.

3. Results and Discussions

3.1. Phase characterization

3.1.1. Microscopic analysis

During the blasting process, it is expected that the abrasives behave only as an agent to generate the wanted profile that will guarantee not only the proper cleaning of the surface (that will posterior receive the coating application) but the necessary roughness to ensure the proper adherence of the coating. The ideal situation is depicted in Figures 3a and 3b. In those cases, the abrasive particle contacts the metal surface, generates the effective "peak-valley" roughness profile and leaves the surface without any material deposited on it. As mentioned before, mainly due to particle fragmentation, abrasive amounts are "trapped" in the surface valleys impairing the corrosion properties of coatings (Figure 3c).

Figure 4 depicts the observation of this type of entrapment in the valleys created over the metal surface. Deposits of fragmented material (2a) and whole abrasive particles (2b) were observed in every surface analyzed. Blasted substrates were microscopic analyzed in order to
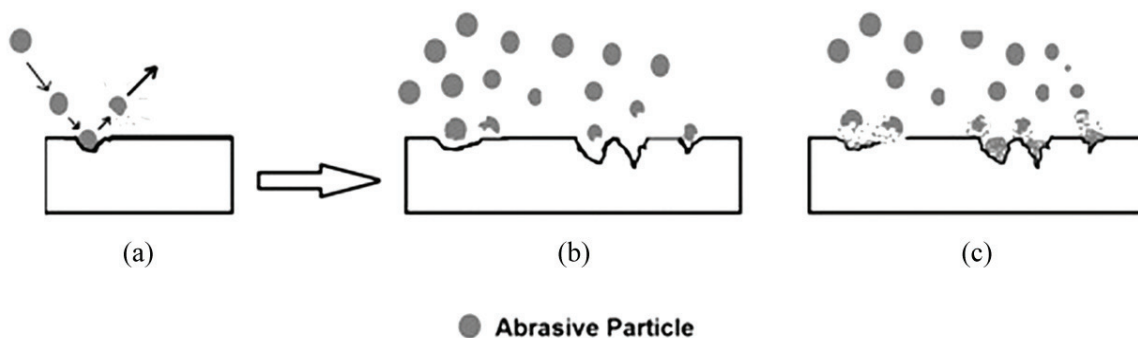

Abrasive Particle

Figure 3. (a-b) Abrasive particles hit the metal substrate surface to generate the desired roughness profile, leaving that surface without any particulate deposit. (c) Abrasive particles fragments deposited over the metal surface.
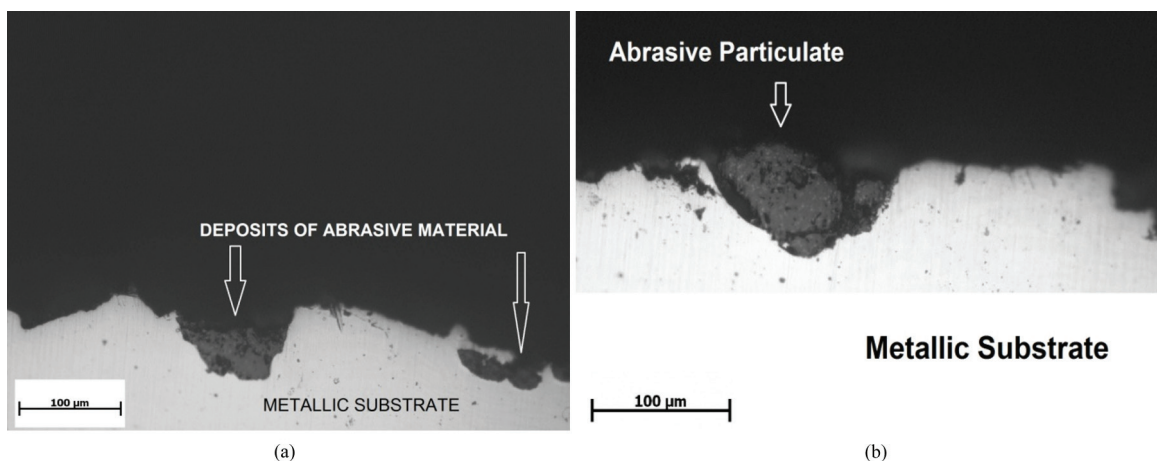

Figure 4. (a) Micrographs of deposits of abrasive material in the valleys created by the particle impact over the surface. (b) Observation of a whole particle entrapped in a valley.

investigate the aspect of the abrasive contamination. The superficial aspect of each blasted substrate obtained after optical examination is shown in Figure 5. It can be observed that the MCS and MSS abrasives generated a rougher surface over both CS and SDS substrate.

3.1.2. X-ray analysis

Diffraction patterns were obtained for both substrate bulks, prior to the blasting process, to work as a reference pattern when measuring the degree of contamination of

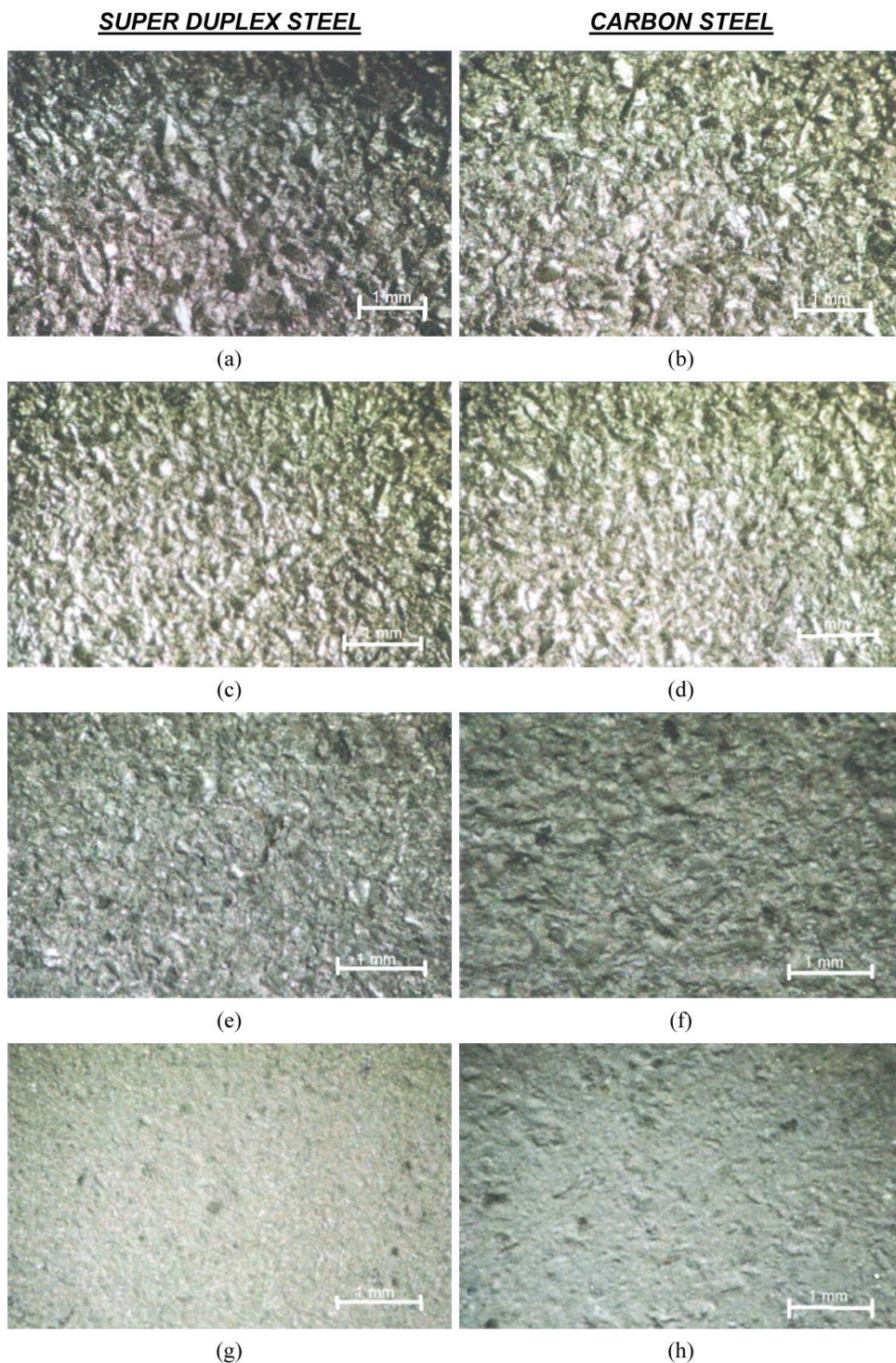**SUPER DUPLEX STEEL**   **CARBON STEEL**

Figure 5. Aspect of each metallic substrate (Super Duplex and Carbon Steel) after abrasive blasting. (a-b) MCS blasting, (c-d) MSS blasting, (e-f) SB blasting and (g-h) DA blasting.

the samples subsequently analyzed. This was particularly important for the case where the martensitic steel abrasive was used, as it served as a reference for identifying the contribution of the abrasive to the substrate of similar crystal structure. The CS substrate indicated the major presence of α-Fe (ferrite) in its internal structure while the SDS substrate revealed α-Fe and γ-Fe (ferrite and austenite, respectively). The structures used as reference for fitting that phases were BCC α-Fe[46], FCC γ-Fe[47].

Regarding the composition of commercial abrasives, a predominance of phase α-Al_2O_3 (alpha alumina) was verified in the SB abrasive while κ-Al_2O_3 (kappa alumina) was the major phase presented in the DA abrasive. Therefore, the structure models used for indexing these phases after blasting were Rhombohedral α-Al_2O_3[48] and Orthorhombic κ-Al_2O_3[49]. The same procedure was made for the martensitic steel abrasive, which indicated peaks for martensite phase, indexed as Tetragonal CFe[50], for both MCS and MSS abrasives.

Figure 6 presents the diffraction patterns for the carbon steel substrate before and after abrasive blasting (a and b) and for the super duplex steel before and after blasting (c and d), respectively.

Observation of both "after blasting" diffraction patterns in Figure 6 indicates the presence of alumina phases in both substrates. It is easy to see the contamination from α-Al_2O_3 originated from the SB abrasive and κ-Al_2O_3 from the DA abrasive, as indicated over the peaks. However, direct observation for the martensitic steel abrasive contamination is not possible as it is for the alumina abrasive. In this case, the most intense peaks of martensite are overlapped by some of the peaks of ferrite (α-Fe) and not directly displayed in the diffractograms. This fact does not hinder the calculations though, as the method can have its parameters adjusted to look for both overlapped phases. That can be done by comparison with the non blasted surfaces spectra. This is another advantage of the Rietveld approach over other X-Ray QPA techniques[25].
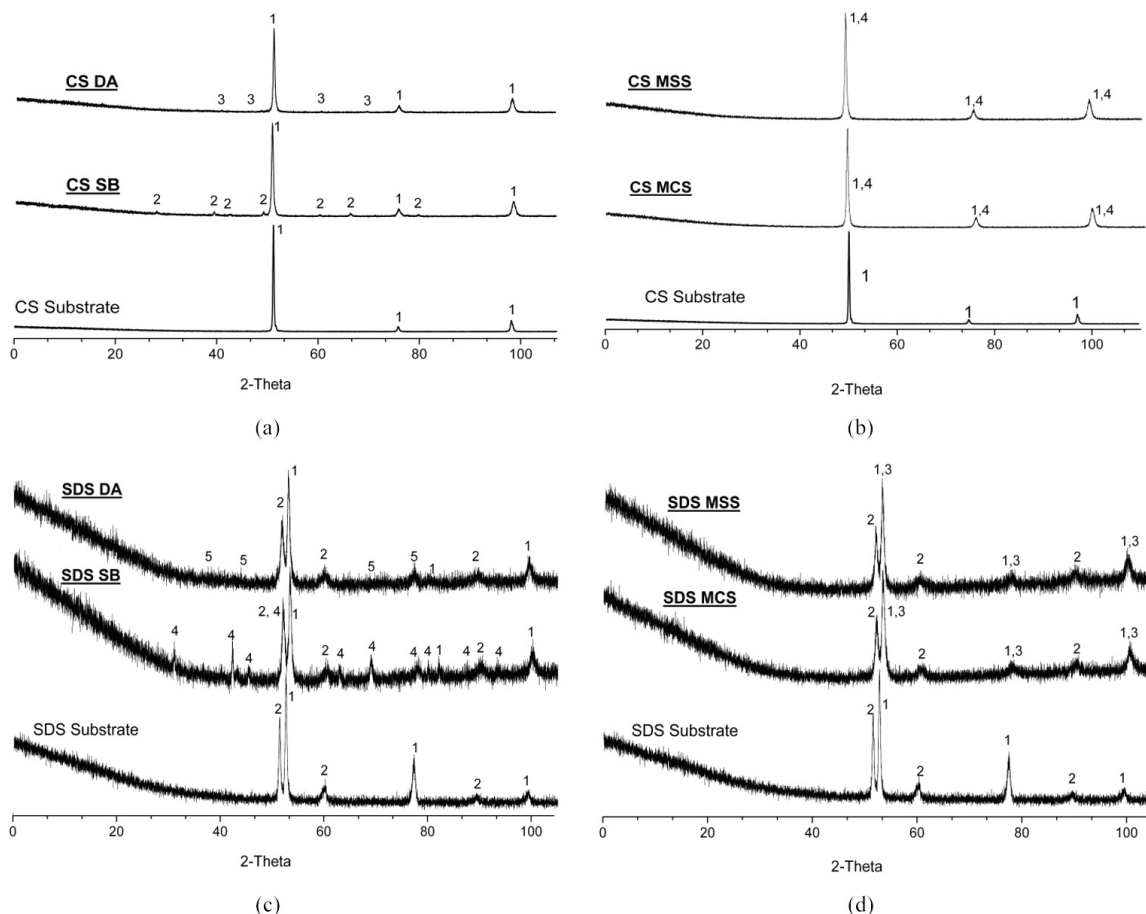

Number	1	2	3	4	5
Phase	Fe-α	Fe-γ	Martensite	α-Al$_2$O$_3$	κ-Al$_2$O$_3$

Figure 6. Diffraction pattern of Carbon Steel (CS) and Super Duplex Steel before and after blasting. Figure 6a indicates the CS after DA and SB blasting and 6b CS after MCS and MSS blasting. Figure 6c indicates the SDS after DA and SB blasting and 6d SDS after MCS and MSS blasting. In both cases where blasting where performed with Al$_2$O$_3$ abrasives, contamination could be clearly seen, whereas for the martensitic steel blasting that contamination was not so evident, as the martensite peaks are coincident with the α-Fe peaks.

Table 5. Fitting criteria for Rietveld calculations - Calculated Goodness of Fitness (GOF) and R-values for blasted substrates.

Abrasive	CS substrate				SDS substrate			
	Rexp	Rwp	Rp	GOF	Rexp	Rwp	Rp	GOF
SB	12.61	14.37	10.48	1.14	9.84	10.33	8.17	1.05
DA	12.83	14.49	10.70	1.13	8.91	9.53	7.36	1.07
MCS	12.93	14.09	10.50	1.09	9.65	10.22	7.93	1.06
MSS	8.32	9.06	9.58	1.09	10.52	11.15	9.92	1.06

Table 6. Results for Rietveld calculations and QPA of CS and SDS substrates blasted with (a) Aluminum Oxide Abrasives (SB and DA) and (b) Martensitic Steel Grit (MCS and MSS). The values indicated the calculated average and standard deviation for the set of 4 substrate pieces used in each blasting.

(a)			
	%Fe-α	%Fe-γ	%Al$_2$O$_3$
Abrasive SB			
Super Duplex	38.79 ± 1.84	25.01 ± 2.13	36.20 ± 2.92
Carbon Steel	79.79 ± 2.37	.	20.21 ± 2.37
Abrasive DA			
Super Duplex	47.31 ± 2.21	36.92 ± 1.16	15.77 ±2.52
Carbon Steel	89.56 ±0.59	.	10.45 ±0.59
(b)			
	%Fe-a	%Fe-g	%Martensite
Abrasive MCS			
Super Duplex Substrate	59.73 ± 1.62	27.52 ± 1.46	12.76 ± 1.21
Carbon Steel Substrate	97.80 ± 0.14	.	2.20 ± 0.14
Abrasive MSS			
Super Duplex Substrate	50.04 ± 0.50	29.97 ± 1.07	20.00 ± 1.27
Carbon Steel Substrate	96.21 ± 1.32		3.79 ± 1.32

Accounting these results, calculation on Topas 4.2 was carried out in order to determine the effective degree of contamination by the abrasives on both substrates. For each substrate, specific parameters were chosen accordingly, with the aim of optimizing each fitting performed.

Table 5 presents the statistics values for each calculation. A GOF factor greater than 1.5 is usually seen as an inadequate model or false minimum, whereas those values lower than 1.0, are, in fact depicting a model that contain more parameters than can be justified by the quality of the data, as insufficient counting time for processing or high influence of background, for example. Therefore, the obtained values are quite satisfactory and a good indication of the efficiency of fitness performed for phase amount calculations, since all of them presented values between 1 and 1.5. Comparing the values for the R factors, it can be observed that, despite Rp and Rwp values differ more than the recommended value of 20%, simulated spectrum curves presented a good correspondence, as seen in Figures 1 and 2.

Table 6 presents the QPA values for the amount of abrasive contamination in both substrates. It can be seen that 36.20% of the average blasted area of SDS substrate was taken by SB particles whereas 20.21% of the average blasted surface of a Carbon Steel (CS) was taken. The same tendency happens for the DA abrasive. 15.77% of the SDS area was taken by abrasive while 10.45% was the percentage of area contaminated in the CS substrate.

In the case of the martensitic abrasive, the SDS once again presents higher degrees of contamination than the CS. For the MS abrasive, SDS substrate presented 12.76% when compared to the CS substrate that indicated 2.20% of contamination. For the MSS abrasive, 20.00% of the SDS area was taken while 3.79% was the percentage for the CS substrate.

The higher percentage of contamination on the SDS substrate can be related with its high hardness. Practical consequences of such higher contamination for the performance of anticorrosive organic coatings are discussed elsewhere[51].

In any case, it could be seen that the Rietveld approach shows to be effective in determining the contamination of metallic substrates blasted with alumina and martensitic steel abrasives.

4. Conclusions

Rietveld quantitative phase analysis (QPA) was able to determine the degree of contamination of abrasives in blasted metallic substrates. The main goal was to create and perform a methodology for addressing this contamination in a trustable way, even when similar phases are present both in the abrasive and in the substrate. The backbone of this methodology consisted in determining the phases presented in each substrate analyzed by X-ray diffraction

and comparing those with simulated peaks constructed by the adequate choice of structural and crystallographic parameters. Then, quantification equations were applied to determine the effective degree of contamination in each different substrate. In order to verify the effectiveness of the fitting, statistic criteria were chosen accordingly. It was observed that SDS revealed a higher degree of contamination when compared to the CS either for alumina abrasives as for martensitic abrasives.

It can be concluded that the Rietveld approach can work as a tool for determining the contamination of metallic blasted substrates. That encourages adoption of the method, taking into account the importance of such contamination on the anticorrosive properties of the alloys and in the performance of organic coatings to be applied on those.

Acknowledgements

References

1. Armas IA and Moreuil SD. *Duplex Stainless Steels*. New Jersey: Wiley; 2009.

2. Bernhardsson S, Oredsson J and Martenson C. *Duplex Stainless Steels*. ASM; 1983.

3. Yamashita M, Matsumoto S and Hironata N. Corrosion resistance and properties of duplex stainless steels. In: International Conference &Expo Duplex Stainless Steels'07; 2007; Italy. 2007

4. Schweitzer PA. *Corrosion Engineering Handbook*. 2nd ed. Florida: CRC Press; 2007.

5. Satas D and Tracton AA. *Coatings Technology Handbook*. 3rd ed. Florida: CRC Press; 2005.

6. Momber A, editor. *Blast Cleaning Technology*. Berlin: Springer; 2008. http://dx.doi.org/10.1007/978-3-540-73645-5.

7. Momber A and Wong YC. Overblasting effects on surface properties of low-carbon steel. *Journal of Coatings Technology and Research*. 2005; 2(6):453-461. http://dx.doi.org/10.1007/BF02733888.

8. International Organization for Standardization – ISO. *ISO 4628-2: Paints and varnishes: evaluation of degradation of coatings: designation of quantity and size of defects and of intensity of uniform changes in appearance: assessment of degree of blistering*. Switzerland; 2003.

9. International Organization for Standardization – ISO. *ISO 8501-1: Preparation of steel substrates before application of paints and related products: visual assessment of surface cleanliness: rust grades and preparation grades of uncoated steel substrates and of steel substrates after overall removal of previous coatings*. Switzerland; 2007.

10. Morcillo M, Bastidas M, Simancas J and Galvan JC. The effect of the abrasive work mix on paint performance over blasted steel. *Anti-Corrosion Methods and Materials*. 1989; 36(5):4-8. http://dx.doi.org/10.1108/eb020755.

11. American Society for Testing and Materials – ASTM. *ASTM E1245-03: Practice for Determining the Inclusion or Second-Phase Constituent Content of Metals by Automatic Image Analysis*. West Conshohocken; 2003.

12. Zevin LS and Kimmel G. *Quantitative X-Ray Diffractometry*. Berlin: Springer; 1995.. http://dx.doi.org/10.1007/978-1-4613-9535-5.

13. Klug HP and Alexander LE. *X-ray diffraction procedures for polycrystalline and amorphous materials*. 2nd ed. New Jersey: John Wiley & Sons; 1974.

14. Cullity BD. *Elements of X-ray diffraction*. 2nd ed. Boston: Addison-Wesley Publishing Company; 1978.

15. Hubbard CR and Snyder RL. RIR - Measurement and use in quantitative XRD. *Powder Diffraction*. 1988; 3(2):74-77. http://dx.doi.org/10.1017/S0885715600013257.

16. Chung FH. Quantitative interpretation of X-ray diffraction patterns of mixtures. I. matrix-flushing method for quantitative multicomponent analysis. *Journal of Applied Crystallography*. 1974; 7(6):519-525. http://dx.doi.org/10.1107/S0021889874010375.

17. Rietveld HM. A profile refinement method for nuclear and magnetic structures. *Journal of Applied Crystallography*. 1969; 2(2):65-71. http://dx.doi.org/10.1107/S0021889869006558.

18. Bish DL and Howard SA. Quantitative phase analysis using the Rietveld method. *Journal of Applied Crystallography*. 1988; 21(2):86-91. http://dx.doi.org/10.1107/S0021889887009415.

19. Bish DL and Chipera SJ. Problems and solutions in quantitative analysis of complex mixtures by X-ray powder diffraction. *Advances in X-ray Analysis*. 1987; 31:295-308.

20. Bish DL and Chipera SJ. Accuracy in Quantitative X-Ray Powder Diffraction Analyses. *Advances in X-ray Analysis*. 1995; 38:47-57.

21. Chipera SJ and Bish DL. Multireflection RIR and intensity normalizations for quantitative analyses: Applications to feldspars and zeolites. *Powder Diffraction*. 1995; 10(1):47-55. http://dx.doi.org/10.1017/S0885715600014305.

22. Snyder RL and Bish DL. Quantitative analysis: modern powder diffraction. In: Bish DL and Post JE, editors. *Reviews in Mineralogy*. Denver: Mineralogical Society of America; 1989. p. 101-144.

23. Suortti P. Effects of porosity and surface roughness on the X-ray intensity reflected from a powder specimen. *Journal of Applied Crystallography*. 1972; 5(5):325-331. http://dx.doi.org/10.1107/S0021889872009707.

24. Bruker. *Topas: general profile and structure analysis software for powder diffraction data*. Karlsruhe; 2003.

25. Young R. *The Rietveld Method*. New York: Oxford University Press; 1995

26. Hill RJ. Calculated X-ray powder diffraction data for phases encountered in lead/acid battery plates. *Journal of Power Sources*. 1983; 9(1):55-71. http://dx.doi.org/10.1016/0378-7753(83)87015-3.

27. Hill RJ and Howard CJ. Quantitative phase analysis from neutron powder diffraction data using the Rietveld method. *Journal of Applied Crystallography*. 1987; 20(6):467-474. http://dx.doi.org/10.1107/S0021889887086199.

28. McCusker LB, Von Dreele RB, Cox DE, Louër D and Scardi P. Rietveld refinement guidelines. *Journal of Applied Crystallography*. 1999; 32(1):36-50. http://dx.doi.org/10.1107/S0021889898009856.

29. Sparks CJ, Kumar R, Specht ED, Zschack P, Ice GE, Shiraishi T, et al. Effect of powder sample granularlity on fluorescent intensity and on thermal parameters in X-ray diffraction rietveld analysis. *Advances in X-ray Analysis*. 1992; 35:57-62.

30. Pitschke W, Hermann H and Mattern N. The influence of surface roughness on diffracted X-ray intensities in Bragg-Brentano geometry and its effect on the structure determination by means of Rietveld analysis. *Powder Diffraction*. 1993; 8(2):74-83. http://dx.doi.org/10.1017/S0885715600017875.

31. Pitschke W, Mattern N and Hermann H. Incorporation of microabsorption corrections into Rietveld analysis. *Powder Diffraction*. 1993; 8(4):223-228. http://dx.doi.org/10.1017/S0885715600019412.

32. Sidey V. A simplified correction function for the effect of surface roughness in X-ray powder diffraction. *Journal of Applied Crystallography*. 2004; 37(6):1013-1014. http://dx.doi.org/10.1107/S002188980402254X.

33. Paiva-Santos CO, Marques RFC, Franco MK, Silva MT and Jafelicci-Jr M. *Surface Roughness Effect on the B's Values in the Rietveld Refinement - The crystal structure of La1-fSrfMnO3(f > 0.35)*. Available from: <http://labcacc3.iq.unesp.br/?p=493>. Acess in: 05/11/2014.

34. American Society for Testing and Materials – ASTM. *ASTM A516: Standard Specification for Pressure Vessel Plates, Carbon Steel, for Moderate- and Lower-Temperature Service*. United States; 2010.

35. American Society for Testing and Materials – ASTM. *ASTM E11 09: Standard Specification for Woven Wire Test Sieve Cloth and Test Sieves*. United States; 2009.

36. American Society for Testing and Materials – ASTM. *ASTM E11 10: Standard Specification for Woven Wire Test Sieve Cloth and Test Sieves*. United States; 2010.

37. Cheary RW and Coelho A. A fundamental parameters approach to X-ray line-profile fitting. *Journal of Applied Crystallography*. 1992; 25(2):109-121. http://dx.doi.org/10.1107/S0021889891010804.

38. Boyd JP. *Chebyshev and Fourier Spectral Methods*. 2nd ed. New York: Dover Publications; 2001.

39. March A. Mathematische Theorie der Regelung nach der Korngestalt bei affiner Deformation. *Zeitschrift fur Kristallographie*. 1932; 81:285-297.

40. Dollase WA. Correction of intensities for preferred orientation in powder diffractometry: application of the March model. *Journal of Applied Crystallography*. 1986; 19(4):267-272. http://dx.doi.org/10.1107/S0021889886089458.

41. Zolotoyabko E. Determination of the degree of preferred orientation within the March-Dollase approach. *Journal of Applied Crystallography*. 2009; 42(3):513-518. http://dx.doi.org/10.1107/S0021889809013727.

42. The European Mathematical Society. *Encyclopedia of mathematics*. Available from: <http://www.encyclopediaofmath.org/index.php?title=Spherical_harmonics,_method_of&oldid=13148>. Acess in: 05/11/2014.

43. Wilson AJC. Structure and statistics in crystallography. In: *Proceedings of the Symposium on Crystallographic Statistics Held in Hamburg*. 1984; Hamburg, West Germany. Hamburg: Adenine Pr; 1985. p. 95-108.

44. Young RA and Wiles DB. Profile shape functions in Rietveld refinements. *Journal of Applied Crystallography*. 1982; 15(4):430-438. http://dx.doi.org/10.1107/S002188988201231X.

45. Young RA, Prince E and Sparks RA. Suggested guidelines for the publication of Rietveld analyses and pattern decomposition studies. *Journal of Applied Crystallography*. 1982; 15(3):357-359. http://dx.doi.org/10.1107/S0021889882012138.

46. Gorton AT, Bitsianes G and Joseph TL. Thermal Expansion Coefficients for Iron and Its Oxides From X-Ray Diffraction Measurements At Elevated Temperatures. *Transactions of the Metallurgical Society of AIME*. 1965; 233(8):1519-1525.

47. Ridley N and Stuart H. Partial Molar Volumes from High-Temperature Lattice Parameters of Iron–Carbon Austenites. *Metal Science Journal*. 1970; 4(1):219-222. http://dx.doi.org/10.1179/msc.1970.4.1.219.

48 Morris MC et al. *Standard X-ray difraction powder patterns*. Washington: US National Bureau of Standards; 1960. p. 3. Circular 539, v. 9.

49. Ollivier B, Retoux R, Lacorre P, Massiot D and Férey G. Crystal structure of κ-alumina: an X-ray powder diffraction, TEM and NMR study. *Journal of Materials Chemistry*. 1997; 7(6):1049-1056. http://dx.doi.org/10.1039/a700054e.

50. Cheng L, Böttger A, Keijser TH and Mittenmeijer EJ. Lattice Parameters of Iron-Carbon and Iron-Nitrogen Martensites and Austenites. *Scripta Materialia*. 1990; 24(3):509-514. http://dx.doi.org/10.1016/0956-716X(90)90192-J.

51. Nascimento AV. *Aspects of Surface Treatments of Super Duplex Stainless Steels for Application of Anticorrosive Coatings*. [Dissertation]. Rio de Janeiro: Universidade Federal do Rio de Janeiro; 2009.